Proc. Natl. Acad. Sci. USA
Vol. 90, pp. 4136–4140, May 1993
Biochemistry

Crystal structure of a ubiquitin-dependent degradation substrate: A three-disulfide form of lysozyme

(proteolysis/ubiquitination/specificity determinant/stability)

CHRISTOPHER P. HILL*, NANCY L. JOHNSTON, AND ROBERT E. COHEN†

Department of Chemistry and Biochemistry and the Molecular Biology Institute, University of California, Los Angeles, CA 90024-1570

Communicated by Howard K. Schachman, January 29, 1993 (received for review December 16, 1992)

ABSTRACT **Covalent attachment of ubiquitin marks substrates for proteolysis, but features that identify ubiquitination targets such as chicken egg white lysozyme are poorly understood. Recognition of lysozyme first requires reduction of Cys-6 Cys-127, one of its four native disulfide bonds, and Cys-6,Cys-127-carboxymethylated (6,127-rcm) lysozyme can mimic this three-disulfide intermediate. The 6,127-rcm form of lysozyme is known to retain a substantially native-like conformation in solution, and we demonstrate that it is this folded structure that is recognized for ubiquitination. Because native lysozyme is not a substrate, differences between the native and three-disulfide structures must include features responsible for selective ubiquitination. The 1.9-Å resolution crystal structure of 6,127-rcm-lysozyme, reported here, affords a view of this ubiquitin-dependent degradation substrate. Two conformers of 6,127-rcm-lysozyme were obtained in the crystal. These differ uniquely from crystal forms of native lysozyme by displacement of the C-terminal residues. The structures suggest that localized unfolding at the C terminus of three-disulfide lysozyme allows the complex of E3α (ubiquitin–protein ligase) and E2 (ubiquitin–carrier protein) to bind to a surface that includes Lys-1 and the putative ubiquitination site Lys-13. From this we infer that the N-terminal and internal substrate recognition sites on the E3α·E2 complex are separated by ≈20 Å.**

Intracellular protein degradation is remarkable for its combination of extreme selectivity and the ability to accommodate an enormous variety of substrates. Protein half-lives *in vivo* span several orders of magnitude. Moreover, mutations, translational errors, mislocalization, and chemical damage all can lead to polypeptides that are rapidly degraded (1–5). How such proteins are distinguished from their long-lived counterparts is largely unknown. In eukaryotes, a major route for intracellular proteolysis involves covalent modification of protein lysine(s) with the protein ubiquitin (Ub) and subsequent degradation by the 26S Ub-dependent protease complex (6–8). Specificity resides, at least in part, with the Ub–protein ligase that marks a substrate for recognition by the protease. This process is best understood for the E3α ligase from rabbit reticulocytes and the related *UBR1*-encoded enzyme from yeast (9–13).

One important E3α recognition determinant is the substrate's N terminus, where only a subset of amino acids is permissive for ubiquitination (9–12). A permissive N terminus is not sufficient, however, and the relative orientations and distances that separate lysine ubiquitination sites from N-terminal and other, as yet undiscovered, determinants also are likely to be critical for recognition (14–17). Progress in this area has been hampered by the lack of Ub-dependent degradation substrates of defined structure. Indeed, to obtain competent *in vitro* substrates, proteins generally must be altered conformationally (16, 17). This generalization applies to chicken egg white lysozyme, where we have found that efficient ubiquitination requires prior reduction of one of the four native disulfide bonds, Cys-6 Cys-127. A reduced and carboxymethylated derivative, 6,127-rcm-lysozyme, can mimic this three-disulfide degradation intermediate (17). Three-disulfide lysozyme offers a unique opportunity to probe ubiquitination specificity because, unlike other E3α substrates described thus far, it retains a substantially structured, native-like conformation (17–19). We report here the x-ray crystal structure of 6,127-rcm-lysozyme determined to a resolution of 1.9 Å. An experiment that relates this structure to the substrate conformation recognized in solution by Ub–protein ligase is presented, and the results are discussed in terms of structural determinants for ubiquitination.‡

EXPERIMENTAL PROCEDURES

Protein Crystallization. The 6,127-rcm derivative of chicken egg white lysozyme (EC 3.2.1.17; Sigma, grade I) was prepared essentially as described (17), but with additional chromatography on a PolyCAT A (The Nest Group, Southboro, MA) cation-exchange column. Stock solutions were dialyzed against water and concentrated to 9 mg/ml in Centricon 10 microconcentrators (Amicon). Crystals were grown by the hanging drop method under conditions similar to those used to obtain tetragonal crystals of unmodified lysozyme. The reservoir solution (1 ml) was 7% NaCl with 50 mM sodium acetate at pH 3.8, and the hanging drops contained 10 μl of a 1:1 mixture of reservoir and protein stock solutions. Typically, crystals appeared after 2 days and grew to 0.3 × 0.4 × 0.5 mm^3 within a week. The crystals belonged to orthorhombic space group $P2_12_12_1$ with cell dimensions a = 77.7 Å, b = 81.3 Å, and c = 38.0 Å.

Data Collection and Structure Determination. X-ray data extending to 1.9-Å resolution were collected from two crystals with a R-AXIS II imaging plate detector and a Rigaku RU-200 rotating anode source (CuKα radiation at 50 kV and 150 mA). Each frame, in which the crystal was oscillated by 1.5°, was acquired over 12 min; ≈35 frames were collected from each crystal before there was significant deterioration from radiation damage. Processing employed the MSC software package. The chicken egg white lysozyme structure of

The publication costs of this article were defrayed in part by page charge payment. This article must therefore be hereby marked "*advertisement*" in accordance with 18 U.S.C. §1734 solely to indicate this fact.

Abbreviations: Ub, ubiquitin; 6,127-rcm, Cys-6,Cys-127-carboxymethylated; rcmA and rcmB, the two molecules per asymmetric unit in 6,127-rcm-lysozyme crystals; E3, ubiquitin–protein ligase; E2, ubiquitin carrier or conjugating protein; $(GlcNAc)_3$, *N,N',N"*-triacetylchitotriose.

*Present address: Department of Biochemistry, University of Utah, Salt Lake City, UT 84132.
†To whom reprint requests should be addressed at: Molecular Biology Institute, University of California, 405 Hilgard Avenue, Los Angeles, CA 90024-1570.

‡Coordinates and diffraction data have been deposited in the Protein Data Bank, Chemistry Department, Brookhaven National Laboratory, Upton, NY 11973 (reference 1RCM) (20, 21).

Strynadka and James (22) was used as a starting model for 6,127-rcm-lysozyme structure determination. Water molecules and side chains with multiple conformations were deleted from the starting model, as were the first 14 and last 6 amino acids. The 6,127-rcm-lysozyme crystals are similar to those of native lysozyme grown under similar conditions, although the latter are of the tetragonal space group $P4_32_12$ with cell dimensions of $a = b = 79.24$ Å and $c = 37.83$ Å (22). The $P2_12_12_1$ space group of the 6,127-rcm-lysozyme is related to $P4_32_12$ by one two-fold rotation axis. Consideration of this symmetry relationship enabled two copies of the truncated native lysozyme molecule to be placed within the 6,127-rcm-lysozyme asymmetric unit. Rigid-body refinement with XPLOR (23) gave an *R* factor of 26.7% against all 3.0- to 8.0-Å data. This solution was confirmed by rotation function and *R* factor searches using XPLOR. One cycle of simulated annealing refinement using the "slow-cool" protocol was followed by cycles of positional and *B* factor refinement, with several rounds of manual map-fitting using the program FRODO (24) implemented on an Evans and Sutherland ESV graphics station (Salt Lake City). The entire asymmetric unit was inspected in difference maps, water molecules were added, and the protein model was rebuilt where appropriate. Data collection and final refinement statistics are in Table 1.

Ub–Protein Conjugation. Ub-activating enzyme (E1) and the 14-kDa Ub carrier protein ($E2_{14K}$) were purified from calf thymus and rabbit reticulocytes, respectively (25, 26), and ubiquitination assays were done essentially as described (17). Each 10-μl reaction mixture in 50 mM Tris·HCl (pH 7.6) contained 2.5 mM dithiothreitol, 2 mM ATP, 5 mM $MgCl_2$, 5 mM phosphocreatine, 30 mU creatine phosphokinase, 3 mU inorganic pyrophosphatase, and a Ub-depleted rabbit reticulocyte extract (21 μg of protein; see ref. 17) supplemented with 5 μg of bovine Ub (Sigma), 57 nM E1, and 38 nM $E2_{14K}$. After a 5-min preincubation at 37°C with 2 μM Ub–aldehyde to prevent conjugate breakdown by endogenous Ub–protein isopeptidases (16), ^{125}I-labeled substrate (0.4 μg) was added and the incubation was continued for 1 hr. Products were visualized after SDS/polyacrylamide gel electrophoresis and autoradiography (17).

RESULTS AND DISCUSSION

The Folded Form of 6,127-rcm-Lysozyme Is a Ubiquitination Substrate. The 6,127-rcm derivative of lysozyme is thermodynamically less stable than unmodified lysozyme (18, 19), which might suggest that it is the unfolded protein that is recognized by the Ub–protein ligase, E3α. We have found that this is not the case. At 37°C under conditions that mimic a ubiquitination assay, a few percent of 6,127-rcm-lysozyme is in an unfolded state (Fig. 1*A*). As with unmodified lysozyme (28), an oligosaccharide ligand can shift this equilibrium to stabilize the folded form of the 6,127-rcm derivative (Fig. 1*A*), but such stabilization has no effect upon lysozyme ubiquitination (Fig. 1*B*). This same result is obtained over a wide range of lysozyme concentrations, where the substrate is well below the apparent K_m of Ub–protein ligase (unpublished data). Thus, the relatively limited structural differences between the folded conformations of native lysozyme and 6,127-rcm-lysozyme must include features used to distinguish ubiquitination targets from other proteins.

Table 1. Data collection and refinement statistics

Parameter	Value
Resolution range, Å	1.9–10.0
No. of reflections	18,295
Completeness, %	93.8
R_{sym}*	0.042
R_{factor}† (all data)	0.185
No. of water molecules included	133
B factor	
Molecule A average, Å^2	24.7
Molecule B average, Å^2	23.9
Solvent average, Å^2	36.3
rms deviations from ideal geometry	
Bond distances, Å	0.014
Bond angles, degrees	2.8
Dihedral angles, degrees	24.3
rms deviation of main-chain bond *B* values, Å^2	1.7

*$R_{sym} = (\Sigma|I_i - I_{av}|)/\Sigma I_{av}$.
†$R_{factor} = (\Sigma||F_{obs}| - |F_{calc}||)/\Sigma|F_{obs}|$.

Crystal Structure of 6,127-rcm-Lysozyme. The 6,127-rcm-lysozyme was crystallized into space group $P2_12_12_1$, different from that of native lysozyme crystals from which high-resolution structure coordinates are available. We were able to solve the structure by molecular replacement with a model

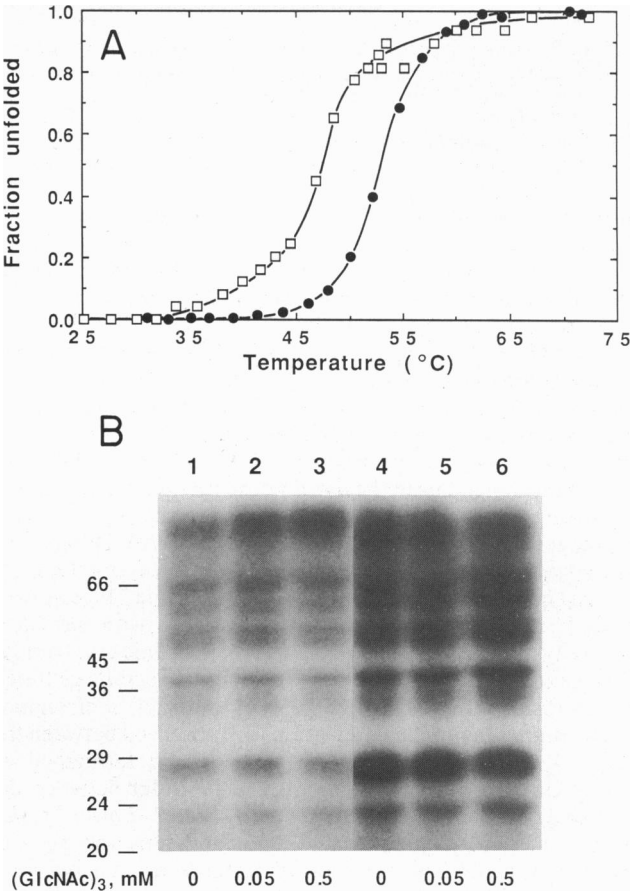

FIG. 1. Ubiquitination of lysozyme does not depend upon global unfolding. (*A*) Thermal denaturation of 6,127-rcm-lysozyme in 50 mM sodium 3-(*N*-morpholino)propanesulfonate buffer (pH 7.0) was monitored by the absorbance change at 280 nm (19), and the data are presented as the fraction of protein in the unfolded state without (□) or with (●) 1.0 mM *N,N',N''*-triacetylchitotriose [$(GlcNAc)_3$]. The ligand stabilizes the protein, increasing its melting transition temperature from 47.6°C to 52.7°C. (*B*) Ub conjugation assays employed ^{125}I-labeled lysozyme (1×10^5 cpm, lanes 1–3) or 6,127-rcm-lysozyme (1.4×10^5 cpm, lanes 4–6) with 0, 0.05, and 0.5 mM $(GlcNAc)_3$ as indicated; native lysozyme and 6,127-rcm-lysozyme under these conditions are saturated by ≥0.05 mM $(GlcNAc)_3$ (ref. 27; unpublished data). Note that by inclusion of 2.5 mM dithiothreitol in these reactions, 1–2% of the native lysozyme is in the three-disulfide form (17). Conjugates (>20 kDa) were visualized after SDS/polyacrylamide gel electrophoresis and autoradiography. Positions of molecular mass markers (kDa) are to the left of the gel; bands corresponding to the ^{125}I-labeled substrates (14 kDa) were overexposed and are not shown.

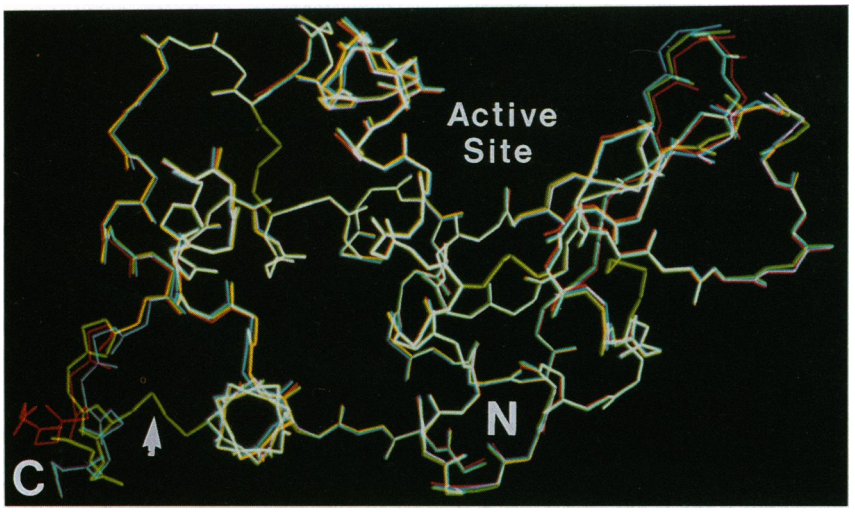

FIG. 2. Comparisons of 6,127-rcm-lysozyme and native chicken egg white lysozyme crystal structures. The main-chain tracing from the 1.75-Å native lysozyme structure (22) is shown in green superimposed upon the two 6,127-rcm-lysozyme conformers (blue and red) determined to 1.9 Å. Where the structures coincide, they appear white; disulfide bonds are shown only for the native structure, and are in green. The C termini, N termini, and active site are indicated. The Cys-6 Cys-127 disulfide, broken in the 6,127-rcm derivative, is identified by the arrow. The Lys-13 ubiquitination site (not shown here; see text) extends from the prominent helix (residues 5–15) that is linked via the Cys-6 Cys-127 disulfide to the C terminus. All three structures are nearly identical except for several residues at the C termini.

of native lysozyme that had been determined from crystals belonging to space group $P4_32_12$ (22). The resultant 1.9-Å resolution atomic model for 6,127-rcm-lysozyme includes two molecules per asymmetric unit and has been refined to an *R* factor of 0.185 (Table 1).

Overall, the conformations of 6,127-rcm-lysozyme and native lysozyme are extremely similar, and significant deviations (i.e., displacements > 1.0 Å) in the polypeptide backbones are limited to only a few regions. Fig. 2 shows the main-chain polypeptide tracings for both of the 6,127-rcm-lysozyme molecules in the asymmetric unit, rcmA and rcmB, superimposed upon the 1.75-Å resolution native lysozyme structure obtained from tetragonal crystals (22). Differences are slight except at the C terminus and, to a lesser extent, for a short peptide segment centered about residue 71 (regions II and IV in Fig. 3 *Upper Left*). Comparisons with the 1.5-Å native lysozyme structure obtained from triclinic crystals (29, 30)[§] revealed deviations for two additional regions centered about residues 47 and 101 (Fig. 3 *Upper Right*). For regions I–III, similar main-chain deviations are observed between the native lysozyme structures (Fig. 3 *Lower Left*, tetragonal vs. triclinic), whereas only regions I and IV differ between the two 6,127-rcm-lysozyme molecules (Fig. 3 *Lower Right*, rcmA vs. rcmB). Positional differences within the pairs of native or 6,127-rcm-lysozyme structures are unequivocal evidence of conformational mobility. Note, however, that region IV of the native lysozyme main chain appears fixed (Fig. 3 *Lower Left*). Thus, upon Cys-6 Cys-127 reduction and carboxymethylation, only the C terminus is seen to deviate from the conformations accessible to lysozyme in the native state.

Although Cys-6 Cys-127 disulfide cleavage frees lysozyme's C terminus from its interaction with the body of the protein, the position of the N-terminal peptide that encompasses Cys-6 is essentially unchanged. An inventory of the contacts in native lysozyme made by residues near the N and C termini shows that this might be expected. Other than the Cys-6 Cys-127 disulfide itself, few interactions stabilize the native conformation of lysozyme's five C-terminal residues, which contribute to only 4 hydrogen bonds as compared to 11 for the first five (N-terminal) residues.

[§]Brookhaven Protein Data Bank reference 2LZT.

Destabilization of the native conformation at the C terminus of 6,127-rcm-lysozyme also must be due in part to electrostatic repulsion of the side chain carboxylates of carboxymethylcysteines 6 and 127. In rcmA and rcmB, residue 127 is oriented to position its side chain into solvent and away from the buried hydrophobic environment of Cys-127 in native lysozyme. These new conformations entail a redirection of the polypeptide backbone, as is evident in Fig. 2. For Cys-6, however, positions of the main-chain and C_β atoms are nearly identical for native lysozyme and 6,127-rcm lysozyme. Placement of the Cys-6 carboxymethyl moieties within the model was precluded by weak electron density, however, which indicates that this side chain is quite mobile.

Conformational Flexibility of the C-Terminal Residues. The conformations of the C-terminal portions of rcmA and rcmB differ significantly from each other and from the native structure. These residues therefore are expected to be mobile in solution, and inspection of lattice contacts suggests that these motions may be much larger when free of the crystalline environment. As illustrated in Fig. 4, the last five residues of 6,127-rcm-lysozyme have contacts to symmetry-related molecules. These contacts are similar for rcmA and rcmB and, in each case, are as extensive as the noncovalent intramolecular interactions. Thus, the deviations of the 6,127-rcm-lysozyme C-terminal residues seen from the crystal structures may severely underestimate the true range of motion in solution.

In contrast, and despite the absence of restrictive lattice contacts (see Fig. 4), the conformations of the N-terminal residues are essentially identical. Two-dimensional NMR measurements by Radford *et al.* (18) support our conclusion that the N-terminal portion of 6,127-rcm-lysozyme is virtually the same as that of the native protein. From an immunochemical study, however, it appeared that the 6,127-rcm-lysozyme N-terminal region may be distorted relative to the native conformation (19). The immunochemical and structural data can be reconciled if the N-terminal epitopes that were probed also included Cys-6 or distal portions of the antigen such as its C terminus.

Recognition by Ub–Protein Ligase. Although movement of the Leu-129 side chain was apparent from the NMR study of 6,127-rcm-lysozyme, whether there was a more extensive rearrangement of the C terminus could not be determined

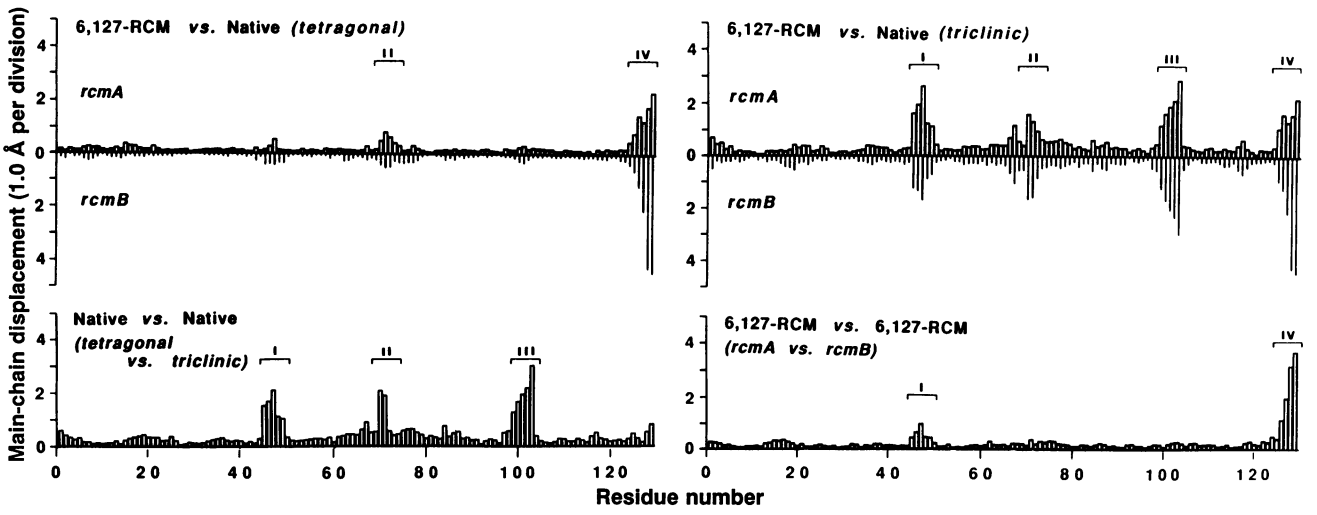

FIG. 3. 6,127-rcm-lysozyme conformation differs uniquely from native lysozyme at its C terminus. Plots of the main-chain rms deviations per residue are shown for all pairwise comparisons of the two 6,127-rcm-lysozyme forms (rcmA and rcmB) and two crystal forms of native lysozyme [tetragonal (22) and triclinic (29, 30)]. For comparisons of 6,127-rcm vs. native forms (*Upper Left* and *Upper Right*), deviations for rcmA are plotted above the horizontal axis and, for rcmB, below the axis. Regions of significant displacement are labeled I–IV. Deviations between the 6,127-rcm and native lysozymes at sites I, II, and III are also seen between the two native forms alone (*Lower Left*) and reflect conformational flexibility within the native protein. However, at the C-terminal five residues (region IV), both 6,127-rcm forms adopt conformations unavailable to native lysozyme.

(18). The crystal structure resolves this issue and points to displacement of the C-terminal segment from its conformation in the native protein as the key alteration that renders three-disulfide lysozyme a ubiquitination target. Substrate recognition by the Ub–protein ligase involves at least two determinants, a permissive N-terminal amino acid and an internal site that may include the ubiquitinatable Lys residue (9–12, 15, 31); these correspond to the E3 "head" and "body" sites postulated by Reiss *et al.* (10, 11). Because accessibility of lysozyme's N terminus (Lys-1) is identical in the 6,127-rcm and native forms, we propose that Cys-6 Cys-127 disulfide cleavage generates a ubiquitination substrate by exposing elements of the second, body site determinant. This site is unlikely to be within the conformationally altered C-terminal region because neither carboxymethylation of Cys-127 nor deletion of Arg-128 and Leu-129 decreases ubiquitination of three-disulfide lysozyme (unpublished work). Instead, as a consequence of the C-terminal rearrangement, there is enhanced exposure of the α-helix delineated by residues 5–15 and which contains Lys-13 as a potential ubiquitination site. Evidence that Lys-13 is the major ubiquitination site has come from experiments with a Lys-13 → Arg mutant form of lysozyme. Unlike the wild-type protein, the Arg-13 variant is ubiquitinated only poorly *in vitro* (unpublished).

Ubiquitination Determinants on Three-Disulfide Lysozyme. A view of the three-disulfide lysozyme surface that presents the N-terminal and putative internal recognition determinants is shown in Fig. 5. The model was constructed from native lysozyme by removal of the Cys-6 Cys-127 disulfide bond and rotation about the N—C_α bond of Gly-126 to swing the C-terminal tetrapeptide into the solvent, as suggested by the 6,127-rcm structures. We propose that this conformational change gives E3α or an E3α·E2 complex access to Lys-13 and allows simultaneous binding to the determinant at the N terminus, Lys-1. This model, in which key binding determinants are accessible only in the locally unfolded molecule, can explain why native lysozyme was unable to compete with the 6,127-rcm derivative in Ub-dependent degradation assays (17). Displacement of the C-terminal residues increases the accessibility of Lys-13 and adjacent residues, particularly Cys-6, Ala-9, and Ala-10, as well as Asp-18 and Leu-25; any or all of these might contribute to a surface for recognition by E3α or an E3α·E2 complex.

In yeast, a flexible polypeptide spacer between the N terminus and Ub attachment site was required for Ub-dependent degradation of modified forms of dihydrofolate reductase and β-galactosidase (15). The need for a minimum spacer length of >5 residues suggested that both determinants may be bound simultaneously to distinct sites on the Ub–protein ligase complex (15). Three-disulfide lysozyme differs from these other model substrates in that the recognition determinants are within a comparatively rigid structure. Indeed, the crystallographic results presented here together with NMR spectroscopy as a probe of solution structure (18) show that in three-disulfide lysozyme the main-chain atom positions are relatively fixed from residue 1 to residue 124. Thus, having demonstrated that E3α recognizes the folded form of three-disulfide lysozyme rather than a transiently unfolded species, we can infer that a distance of ≈20 Å separates the N-terminal and internal sites (i.e., head and body sites) on the mammalian E3α Ub–protein ligase.¶ Other constraints upon substrate recognition are likely to involve residues in the vicinity of Lys-13, and E2 bound to E3α also may participate in these interactions. The 6,127-

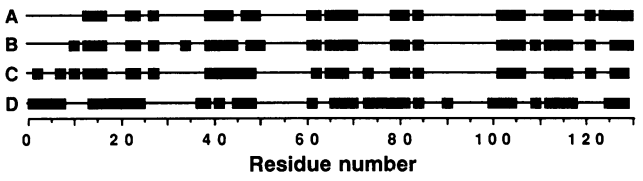

FIG. 4. Intermolecular contacts in the crystal lattice for native and 6,127-rcm lysozymes. Intermolecular contact distances were measured for four lysozyme structures, 6,127-rcm [rcmA (*A*) and rcmB (*B*)] and native [tetragonal (*C*) and triclinic (*D*)]. Superimposed upon lines representing the lysozyme primary sequence, the bars indicate residues ≤4.0 Å away from a symmetry-related protein molecule in the crystal lattice.

¶This distance applies only to the "Type I" N-terminal site that accommodates the basic amino acid Lys, Arg, or His (10–12). Results from the *in vivo* experiments of Bachmair and Varshavsky (15) may reflect proximity of the ubiquitination site to a "Type II" N-terminal site (bulky hydrophobic amino acid) on the yeast enzyme.

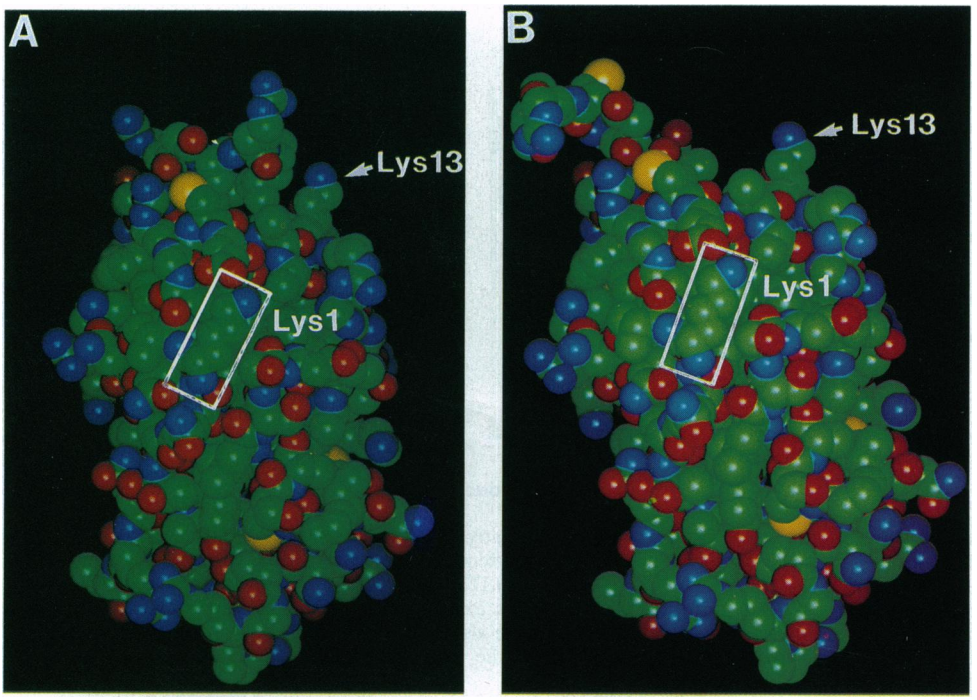

FIG. 5. Unmasking of E3α Ub–protein ligase recognition determinants on lysozyme by Cys-6 Cys-127 disulfide cleavage. Rearrangement of the C terminus in three-disulfide lysozyme was modeled from the native structure (22) by elimination of the Cys-6 Cys-127 disulfide bond and rotation about the N—C_α bond of Gly-126. The spacefilling models depict lysozyme before (*A*) and after (*B*) the disulfide cleavage and bond rotation. The cleft formed by rearrangement of the C-terminal peptide may allow binding of the Ub–protein ligase complex and give access to Lys-13. Side chains for Lys-1 and Lys-13 are indicated, and the C, O, N, and S atoms are colored green, red, blue, and yellow, respectively.

rcm-lysozyme structure will assist in the design of peptide and protein probes to better define these specificity determinants.

We thank J. Setsuda for samples of 6,127-rcm-lysozyme, N. Strynadka and M. James for coordinates to native lysozyme, and D. Eisenberg for his support. This work was supported by National Institute of General Medical Sciences Grant GM 37666 to R.E.C., GM 31299 to the UCLA Structure Group, and Cell and Molecular Biology Training Grant GM 07185.

1. Goldberg, A. L. & St. John, A. C. (1976) *Annu. Rev. Biochem.* **45,** 747–803.
2. Olson, T. S. & Dice, J. F. (1989) *Curr. Opin. Cell Biol.* **1,** 1194–1200.
3. Rivett, A. J. (1990) *Curr. Opin. Cell Biol.* **2,** 1143–1149.
4. Stadtman, E. R. (1990) *Biochemistry* **29,** 6323–6331.
5. Goldberg, A. L. (1992) *Eur. J. Biochem.* **203,** 9–23.
6. Finley, D. & Chau, V. (1991) *Annu. Rev. Cell Biol.* **7,** 25–70.
7. Varshavsky, A. (1992) *Cell* **69,** 725–735.
8. Hershko, A. & Ciechanover, A. (1992) *Annu. Rev. Biochem.* **61,** 761–807.
9. Gonda, D. K., Bachmair, A., Wünning, I., Tobias, J. W., Lane, W. S. & Varshavsky, A. (1989) *J. Biol. Chem.* **264,** 16700–16712.
10. Reiss, Y., Kaim, D. & Hershko, A. (1988) *J. Biol. Chem.* **263,** 2693–2698.
11. Reiss, Y. & Hershko, A. (1990) *J. Biol. Chem.* **265,** 3685–3690.
12. Heller, H. & Hershko, A. (1990) *J. Biol. Chem.* **265,** 6532–6535.
13. Bartel, B., Wünning, I. & Varshavsky, A. (1990) *EMBO J.* **9,** 3179–3189.
14. Hershko, A., Heller, H., Eytan, E. & Reiss, Y. (1986) *J. Biol. Chem.* **261,** 11992–11999.
15. Bachmair, A. & Varshavsky, A. (1989) *Cell* **56,** 1019–1032.
16. Dunten, R. L. & Cohen, R. E. (1989) *J. Biol. Chem.* **264,** 16739–16747.
17. Dunten, R. L., Cohen, R. E., Gregori, L. & Chau, V. (1991) *J. Biol. Chem.* **266,** 3260–3267.
18. Radford, S. E., Woolfson, D. N., Martin, S. R., Lowe, G. & Dobson, C. M. (1991) *Biochem. J.* **273,** 211–218.
19. Denton, M. E. & Scheraga, H. A. (1991) *J. Protein Chem.* **10,** 213–232.
20. Bernstein, F. C., Koetzle, T. F., Williams, G. J. B., Meyer, E. F., Jr., Brice, M. D., Rodgers, J. R., Kennard, O., Shimanouchi, T. & Tasumi, M. (1977) *J. Mol. Biol.* **112,** 535–542.
21. Abola, E., Bernstein, F. C., Bryant, S. H., Koetzle, T. F. & Weng, J. (1987) in *Crystallographic Databases—Information Content, Software Systems, Scientific Applications*, eds. Allen, F. H., Bergerhoff, G. & Sievers, R. (Data Commission of The International Union of Crystallography, Bonn), pp. 107–132.
22. Strynadka, N. C. J. & James, M. N. G. (1991) *J. Mol. Biol.* **220,** 401–424.
23. Brünger, A. T. (1992) XPLOR Manual (Yale Univ., New Haven, CT), Version 3.0.
24. Jones, T. A. (1985) *Methods Enzymol.* **115,** 157–171.
25. Pickart, C. M. & Vella, A. T. (1988) *J. Biol. Chem.* **263,** 12028–12035.
26. Chen, Z. & Pickart, C. M. (1990) *J. Biol. Chem.* **265,** 21835–21842.
27. Banerjee, S. K. & Rupley, J. A. (1973) *J. Biol. Chem.* **248,** 2117–2124.
28. Pace, C. N. & McGrath, T. (1980) *J. Biol. Chem.* **255,** 3862–3865.
29. Hodson, J. H., Brown, G. M., Sieker, L. C. & Jensen, L. H. (1990) *Acta Crystallogr. Sect. B Struct. Sci.* **46,** 54–62.
30. Ramanadham, M., Sieker, L. C. & Jensen, L. H. (1990) *Acta Crystallogr. Sect. B Struct. Sci.* **46,** 63–69.
31. Chau, V., Tobias, J. W., Bachmair, A., Marriott, D., Ecker, D. J., Gonda, D. K. & Varshavsky, A. (1989) *Science* **243,** 1576–1583.